Proceedings of the Combustion Institute, Volume 28, 2000/pp. 1973–1979

EXPERIMENTAL AND COMPUTATIONAL STUDY OF TEMPERATURE, SPECIES, AND SOOT IN BUOYANT AND NON-BUOYANT COFLOW LAMINAR DIFFUSION FLAMES

KEVIN T. WALSH, JOSEPH FIELDING, MITCHELL D. SMOOKE AND MARSHALL B. LONG

Yale University
Department of Mechanical Engineering
New Haven, CT 06520-8284, USA

In this study, we extended previous numerical and experimental investigations of an axisymmetric laminar diffusion flame to assess the role of buoyancy and dilution in flame properties such as temperature, fuel and oxygen concentration, and soot volume fraction. Measurements were made both in normal gravity and on the NASA KC-135 reduced-gravity aircraft. Computations of temperature and major species were performed with a two-dimensional, axisymmetric flame model using a 26-species C_2 hydrocarbon mechanism. This set of temperature and major species measurements affords the most extensive set of comparisons with flame computations to date. Results indicate that the predicted temperature profiles are in excellent agreement with measurement in both normal gravity and microgravity flames at low dilution levels. In these well-predicted flames, however, subtle differences existed in fuel/air mixing between measurement and computation, in which the contrast was most visible in normal gravity. As the fuel stream was diluted, the computations began to lose their predictive ability, again most markedly in normal gravity.

Additionally, relative soot volume fraction was measured with laser-induced incandescence (LII) in both normal gravity and in the time-varying gravitational field provided by the KC-135. Results indicate that the soot concentration and distribution are extremely sensitive to the "g-jitter" present, and that the peak soot volume fraction can increase by as much as a factor of 15 in the absence of gravity.

Introduction

Early laminar flame work in microgravity largely focused on attached jet flames burning in quiescent air and often involved video and thermocouple or probe measurements [1–3]. Many investigated flames could not easily be modeled, given the ill-defined temperature and velocity boundary conditions. Additionally, the qualitative nature of video images and the disrupting flow-field effects of thermocouples and probes presented difficulties in interpreting experimental flame characterizations. In this work, a lifted axisymmetric laminar diffusion flame, which has been well characterized previously both experimentally and computationally in normal gravity, is studied in a microgravity environment. Two-dimensional laser diagnostic techniques such as Rayleigh and Raman scattering, normally restricted to a laboratory environment, were extended to the microgravity environment of the KC-135 reduced-gravity aircraft. This work expands the scope of previous research by allowing comparisons of temperature, species, and soot over a range of flow conditions and gravity levels to lead to a more detailed understanding of the interaction of convection, diffusion, and chemistry in both buoyant and nonbuoyant environments.

The flame under investigation consisted of nitrogen-diluted methane fuel surrounded by an air coflow. In normal gravity, several combined computational/experimental studies were performed on this flame [4–8]. Modeling work employed different kinetic schemes, including a 26-species C_2 hydrocarbon mechanism [5] and GRI Mech 2.11 [9]. Both produced excellent agreement for temperature and major species [7] as well as for trace species such as CH, OH, and NO [5,6,8].

Temperature and major species measurements allowed characteristics such as flame length and liftoff, flamefront curvature, and fuel/air mixing to be quantified over a wide range of fuel dilution levels. Given that fuel composition affects flame chemistry and that buoyancy influences the velocity profile of the flow, we had the opportunity to study the chemistry and fluid dynamic interaction over a wide range of flame conditions. The microgravity environment consequently facilitated a broad set of comparisons between experiment and computation.

Two-dimensional laser imaging techniques such as Rayleigh and Raman scattering are difficult to perform in microgravity facilities due to experimental size, weight, and power requirements. In the last few years, highly compact, pulsed Nd:YAG lasers have become available to alleviate some of these problems. However, many practical issues remain in

making such measurements on the KC-135 reduced-gravity aircraft, among them spurious light scattering in Rayleigh measurements and possible flame fluctuations as a result of g-jitter. In addition, although a computational soot model does not currently exist for this flame, two-dimensional laser-induced incandescence (LII) measurements were made, both in normal gravity and microgravity, to quantify changes in soot concentration and distribution when the influence of gravity was removed. In this case as well, flame stability during a given low-g maneuver was a concern. With all these issues in mind, this work describes two-dimensional temperature, major species, and soot measurements performed on the KC-135. Results from the computations and experiments are presented in the following sections.

Burner Configuration

The burner used in this experiment contained a central fuel jet (4 mm inner diameter, 0.4 mm wall thickness) surrounded by coflowing air (50 mm inner diameter). The standard flow conditions, which have been measured and modeled extensively in normal gravity, consisted of fuel composed of 65% CH_4 diluted with 35% N_2 by volume (denoted 65/35 in later discussion). The exit velocity of both fuel and coflow was 35 cm/s. These conditions produced a blue flame roughly 3 cm in length with a liftoff height of 5.5 mm in normal gravity. A wide range of flow conditions was measured in this study, with the CH_4/N_2 fuel composition varied from 100% CH_4 (denoted 100/0) to 30% CH_4 (denoted 30/70) in 5% increments, with fuel and air exit velocities held fixed at 35 cm/s.

Computational Approach

The computational model used to compute the temperature field, velocities, and species concentrations solved the full set of elliptic two-dimensional governing equations for mass, momentum, species, and energy conservation on a two-dimensional mesh [6]. The resulting nonlinear equations were then solved on an IBM RS/6000 Model 590 computer by a combination of time integration and Newton's method. The chemical mechanism employed was a simple 26-species C_2 hydrocarbon mechanism developed at Yale [5].

Flame structure was calculated over a range of flow conditions in both microgravity and normal gravity. The results of a computed solution at standard flow conditions (65/35) and normal gravity were used as a starting point. In subsequent calculations, the value of the gravitational acceleration (g) was reduced by 10 cm/s^2 and a new solution calculated using Newton's method. A range of flow conditions was reached by using the 65/35 flame as an initial condition and using a similar iterative procedure, varying the fuel mixture in 5% increments.

The 26-species C_2 mechanism utilized in this work showed better agreement with measured liftoff than GRI Mech 2.11 at the 65/35 flow condition. Computations were performed for CH_4/N_2 mixtures ranging from 30/70 to 75/25. However, calculations were not performed at flow conditions less dilute than 75/25, since these flames were observed to produce soot, which was not included in the computational model.

Experimental Setup

Several modifications to the laboratory-based experimental configuration were required to make flame measurements aboard the KC-135 reduced-gravity aircraft. The burner and ignition system were housed inside a pressure vessel maintained at standard atmospheric pressure. The vessel contained three windows, which provided optical access to the flame as well as laser beam entry and exit. The combustion vessel and all measurement equipment were contained within the experiment rig, which was an experimental drop frame provided by the NASA Glenn Research Center. In this rack was a cooled charge-coupled device (CCD) detector and an image intensifier used to measure laser scattering, as well as a color video camera, used to give qualitative insight into flame structure and soot production. The experimental rack also housed the fuel supply, mass flow controllers and power supply, and relays allowing computer control of various components. An external control rack contained a microcomputer system to regulate and monitor experimental systems, along with a VCR and video monitor. A third rack contained a compact, high-power pulsed Nd:YAG laser (Big Sky CFR 400), which required its own mount and associated equipment. This laser produces up to 220 mJ per pulse in the green (at 532 nm) and operates at 10 Hz. The 532 nm beam was shaped, steered through a window, and brought to a focus over the burner centerline. A three-axis accelerometer was mounted directly to the experiment rack to provide a measure of gravitational fluctuations. All equipment racks were bolted to the floor of the aircraft.

Pressure at the vent of the pressure vessel will range from atmospheric pressure at sea level (when the aircraft is on the ground) to nearly 0.2 atmospheres (aircraft at maximum altitude). To keep the combustion vessel at standard atmospheric pressure for all these conditions, an orifice plate and a computer-controlled servo valve were utilized in parallel. This exhaust system kept the combustion vessel pressure at standard atmospheric pressure to better than 1% for the duration of the flight.

Measurements and Image Processing

Temperature measurements were inferred from Rayleigh scattering, which is an elastic light scattering mechanism that can be used to measure number density. The Rayleigh signal at a given point is directly proportional to number density and Rayleigh cross section of the gas mixture at that point [10]. Since our measurements took place at atmospheric pressure, the ideal gas law could be used to relate number density to temperature.

Single-shot Rayleigh measurements were made, which determined non-sooting flames to be stable under the influence of "g-jitter" at the flow conditions measured. Accordingly, the temperature field could be reliably measured with a 100-shot integration, with beam dimensions of 10 mm $\times$ 300 μm, a beam energy of 100 mJ per pulse, and an intensifier gate time of 2 μs. The imaged region extended radially from the jet centerline out to ambient air. An interference filter (532 nm center, 10 nm bandwidth) was used in the collection optics to discriminate against flame luminosity.

At a given height above the burner surface, three measurements were made to produce a background- and response-corrected Rayleigh signal [11]. The central portion of the beam, 8 mm tall, was selected at each height, and the corrected images from seven downstream locations were tiled together to form the measured Rayleigh signal.

These corrected Rayleigh signals were then inverted to form an initial temperature image, where the Rayleigh cross section was assumed to be spatially constant and the temperature in ambient air was set to 300 K. A certain amount of structure or "stripiness" could be seen in these images due to non-uniformities in the laser beam. Since the measured quantity was known to be continuous, a "stripe correction" was done to account for variations in beam structure. This procedure resulted in a smooth, continuous temperature field, which did not change the mean values of these measurements [12].

The spatial variation of the Rayleigh cross section was then taken into account. Major species profiles were computed over a wide range of flow conditions and gravity levels, which allowed the Rayleigh cross section to be determined as a function of temperature in the flames. This double-valued function was then utilized with the stripe-corrected initial temperature profile to account iteratively for spatial variations in the Rayleigh cross section. A self-consistent temperature distribution was reached after five or six iterations. These final images were reflected about the jet centerline to produce the full measured temperature field.

Measurements were made over a wide range of flow conditions and buoyancy levels, from nearly sooting flames (75/25) to the normal gravity blowoff limit (40/60) down to the microgravity blowoff limit (30/70). Note that aboard the KC-135, flames more dilute than 50/50 strained out during the high-g pullout portion of each parabola, requiring the flame to be lit at the start of each low-g portion of the maneuver. Thermometry measurements were made in highly sooting flames (100/0) as well but were not easily interpreted, since computed Rayleigh cross sections as a function of temperature were not available in these flames and soot scattering overwhelmed the Rayleigh signal in certain areas of the flame.

Raman scattering, a weak, inelastic process, was used to measure methane and oxygen concentrations. For these measurements, the laser beam was focused into line (300 μm beam waist) with the laser at full power, 220 mJ per pulse at 532 nm. The Raman signal was imaged along the laser line in two distinct spectral regions at separate times. The first measurements used a 630 nm center, 10 nm bandpass filter to measure methane Raman. The second set utilized a 590 nm center, 10 nm bandpass filter to measure oxygen Raman. The 10 nm spectral region centered on the oxygen Raman peak also included a significant interference from methane Raman scattering. After measurements were made in both spectral regions, the appropriately scaled methane measurement was subtracted from the (O_2 + CH_4) measurement to result in a measured oxygen profile. In both measurements, a uniform concentration of nitrogen was imaged at each height to determine background levels, while a full field of methane or air (as appropriate) was used to determine detector response and to calibrate flame measurements. The temperature variation of the Raman cross section was not accounted for in these number density determinations, since O_2 and CH_4 existed over a modest temperature range and the spectral window was broad. Aboard the KC-135, signals were collected at 30 heights with an integration of 100 shots. For laboratory measurements, data were taken at 150 heights, with the (O_2 + CH_4) signal integrated over 600 shots and the methane signal over 200 shots to improve the signal-to-noise ratio.

Laser-induced incandescence (LII) measurements were made with the 532 nm laser shaped into a 12 mm sheet for maximum spatial coverage. A blue-additive filter, which transmitted roughly 90% between 400 nm and 450 nm, was used in the detection system. For all sooty flames studied in normal gravity and microgravity, the LII signal was measured as a function of laser intensity to ascertain an optimum per pulse energy for the determination of soot volume fraction. Since the soot field was observed to fluctuate during "g-jitter" on the KC-135, the LII images taken in microgravity were single shot. These time-resolved images were indexed with the local acceleration to assess the behavior of these flames in an unsteady gravitational field. Flame luminosity background measurements were made in

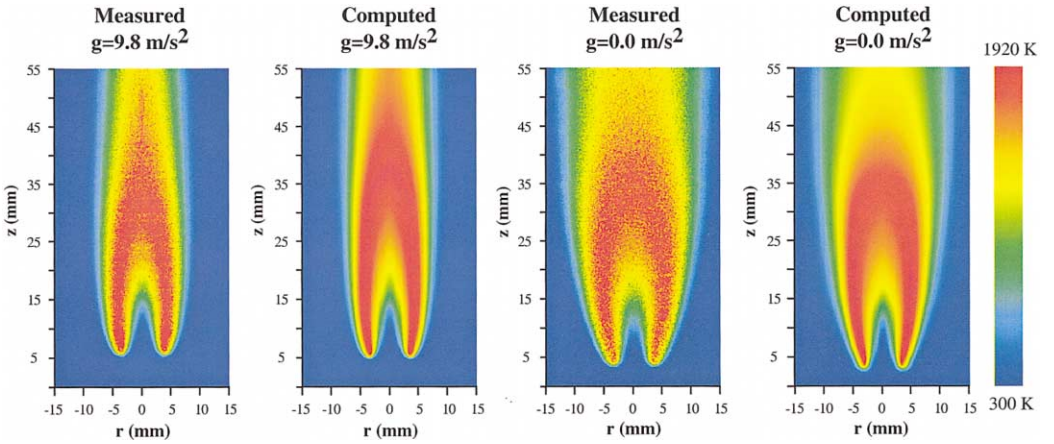

FIG. 1. Measured and computed temperature profiles in the 65/35 flame.

microgravity but could not be subtracted from measured LII signals due to the unsteadiness present in the flames. Single-shot LII measurements were made successfully in the 100% CH_4 (100/0) flame, where five measurements were made during a given low-g parabola. For normal gravity measurements, the soot levels present in methane flames were insufficient to allow for single-shot measurements, so a 100-shot integration was used.

Results and Discussion

The first measurement of these flames focused on the standard flow conditions (65/35) to investigate the role of buoyancy in this extensively characterized flame. Measured and computed temperature distributions in the 65/35 flame are directly compared in Fig. 1. Excellent agreement in flame structure and liftoff height can be seen in the normal gravity flame. In the microgravity flame, we see the computations successfully predict that when the influence of gravity is removed, the high-temperature zone becomes shorter and wider. Stray light reflections prohibited measurements less than 4 mm above the burner surface, but that was sufficient to resolve the flame anchoring region. Measured and computed temperatures are compared more quantitatively in Fig. 2, where the centerline temperature profiles are plotted for this 65/35 flame in both 1*g* and 0*g*. In the normal gravity flame, agreement in liftoff and peak temperature is good, although the flame length is somewhat overpredicted. Agreement in the nonbuoyant flame is excellent—flame liftoff, the lower peak temperature, and shorter flame length are all well predicted.

As nitrogen was added to the fuel stream in 5% increments (by volume), the normal gravity blowoff

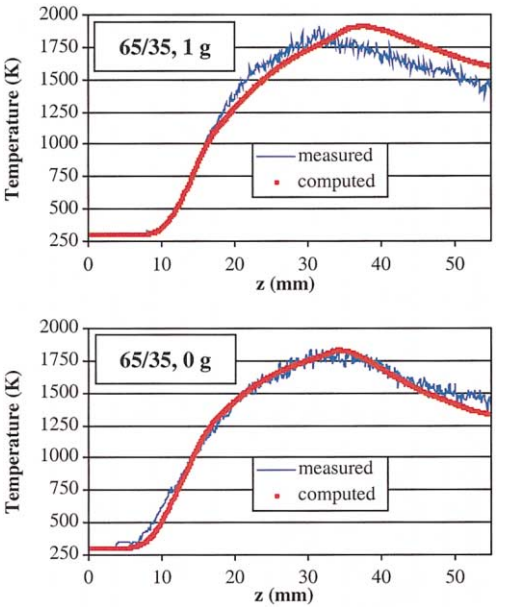

FIG. 2. Measured and computed centerline temperatures in the 65/35 flame.

limit was reached at the 40/60 flow condition. Temperature fields were then measured and computed at this experimental limit, as can be seen in Fig. 3. The normal gravity flame is highly lifted, in strong disagreement with computational prediction. This discrepancy exists to a lesser extent in the microgravity flame. In both normal gravity and microgravity, the computed peak centerline temperature is higher than the measurement by 40 K, which is within measurement error. In microgravity, a temperature profile can be measured at 35/65 as well as

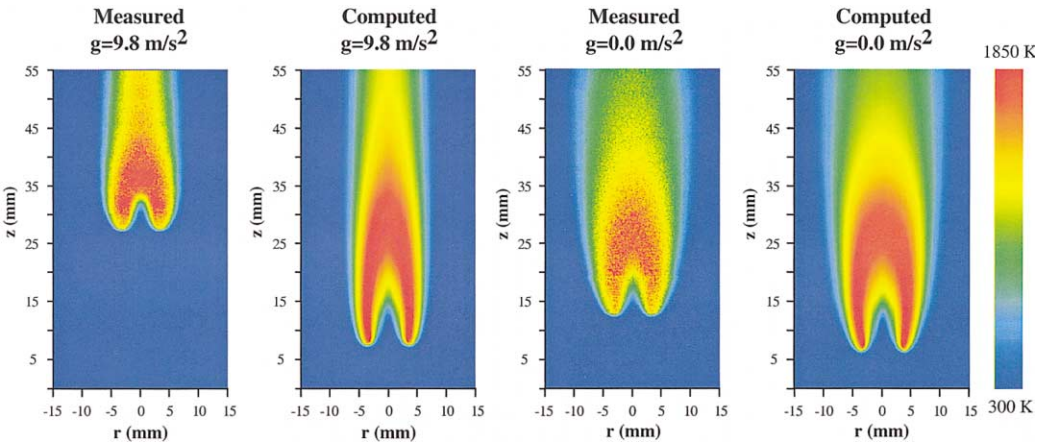

FIG. 3. Measured and computed temperature profiles in the 40/60 flame.

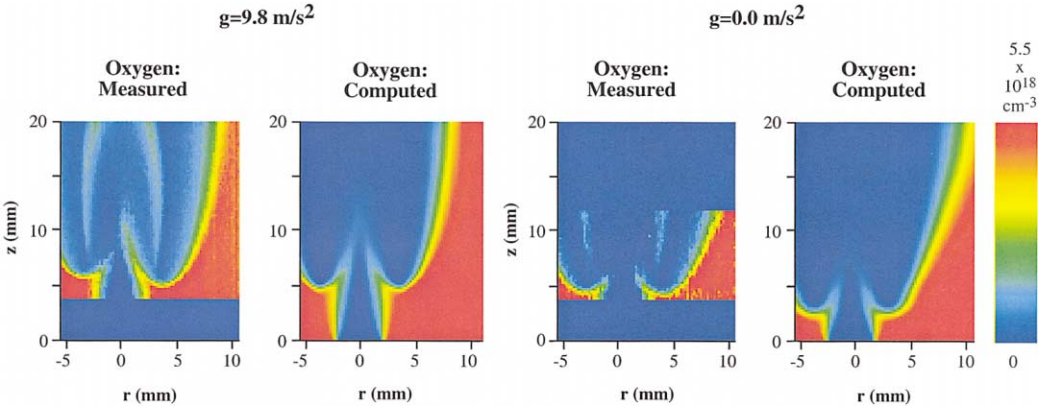

FIG. 4. Measured and computed oxygen profiles in the 65/35 flame.

30/70, the microgravity blowoff limit aboard the KC-135. Though the 35/65 flame was stable, the 30/70 flame moved 1 to 2 mm during a given low-g maneuver. Accordingly, the measured 30/70 profile was spatially averaged, which yielded artificially low temperatures. This flame is extremely flat, faint, and highly lifted, anchoring roughly 37 mm above the burner surface. At this flow condition, the low-noise microgravity environment of the space station may be required to provide a flame stable enough to allow for quantitative, multishot measurements.

Fuel and oxygen Raman measurements were performed in both microgravity and normal gravity at the 65/35 and 40/60 flow conditions. These conditions were chosen to study air/fuel mixing in a flame that was well predicted (65/35) and in a dilute flame where the computational model had less predictive ability. The predicted and measured oxygen profiles are shown for the 65/35 flame in Fig. 4. In the measured normal gravity image, a left-right flame asymmetry can be seen—the flame anchors in a slightly different location on either side of the jet centerline, while the computations assume perfect axisymmetry. In comparing measured and computed O_2 profiles, the characteristics of the "hornlike" structure of air being entrained into the fuel stream are of particular interest. At this "standard" flow condition in normal gravity, this structure compares well on one side but not the other. On the right side of the measured flame is a plume of oxygen which is more concentrated and extends further downstream than any predicted by the computation. In microgravity, however, the measured flame is essentially symmetric, with the behavior at the fuel/oxygen interface well predicted by computation. Note that in both measured oxygen images, a fluorescence interference can be seen in the O_2-free hot zone region.

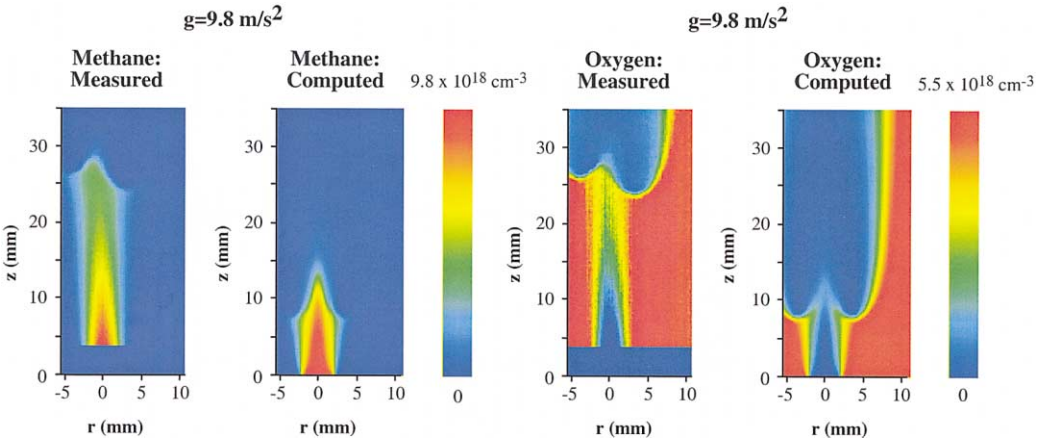

FIG. 5. Methane and oxygen profiles in the 40/60 flame.

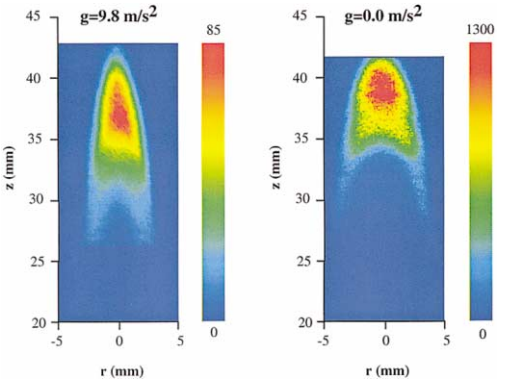

FIG. 6. Relative soot volume fraction measurements in the 100/0 flame.

For the 40/60 flow condition, fuel/air mixing discrepancies between measurement and computation were greatest in normal gravity. This can be seen in Fig. 5, where the 1*g* methane and oxygen distributions are shown. In the measured flame, the fuel travels far downstream until flame stabilization occurs. Raman scattering measures a relatively uniform methane concentration just before the flame anchoring region, where the computations predict steep radial concentration gradients. Furthermore, in the measured flame, a significant amount of oxygen mixes with the fuel before ignition occurs. Because of the discrepancy in the liftoff height, the computations show much less partial premixing. This set of measurements illustrates the experimental sensitivity of these dilute flames to slight flow asymmetries. (Note that the temperature measurements were reflected about the jet centerline and therefore will agree with the species measurements on only one side for these dilute flames.)

The temperature and major species measurements agreed well with computation at moderate fuel dilution levels, while large discrepancies existed for dilute fuel mixtures in terms of flame structure, liftoff, and fuel/air mixing. Although a detailed understanding of these discrepancies requires further investigation, it is clear that the point at which flame stabilization occurs is strongly influenced by chemistry. This was shown in previous work [8], where the computed liftoff height of the 65/35 flame was 1.5 mm lower with GRI Mech 2.11 [9] than with the simpler chemical kinetic mechanism used in this study [5].

In making LII measurements on the KC-135, single-shot measurements were repeated in multiple locations to assess the fluctuations in soot volume fraction and distribution in relation to the time-varying local acceleration. In a given 15 mm region above the burner surface, the peak soot volume fraction varied by as much as 50% over the course of a low-g parabola. However, the measured soot concentration and distribution was repeatable for measurements made during similar g-levels and "g-histories." Therefore, the distribution which resulted after a long (3 s) period of $g = 0$ was considered to be the "best available" soot measurement in the noisy gravitational field available aboard the KC-135. The measured soot distribution in normal gravity and this best available microgravity measurement are shown together in Fig. 6. When the influence of gravity is removed, the (uncalibrated) peak soot volume fraction increase by a factor of 15 while the soot-containing region contracts axially and expands radially. These measurements will be compared with the predictions of computations to assess the validity of existing soot models. Additionally, a low-noise microgravity environment with long timescales may be necessary to allow the flame to reach steady state, as observed in sooty flames by other researchers [3].

In conclusion, temperature, oxygen and methane concentration, and relative soot volume fraction were successfully measured in coflow laminar diffusion flames in both normal gravity and microgravity. When steady, low-soot flames can be established in microgravity the temperature measurements made are as accurate in microgravity as in 1*g*. Although microgravity constraints limited the spatial region measured and the signal-to-noise ratio relative to laboratory major species measurements, the microgravity images obtained allowed many features of air/fuel mixing to be compared with computation. In sum, these temperature and major species measurements afford the most rigorous set of comparisons with flame computations to date. Soot measurements have also been made in 1*g* and 0*g*, which await calibration and comparison with future computational predictions.

Acknowledgments

The support of NASA under Grant NAG3-1939 is gratefully acknowledged, as is the experimental work of summer student Richard Mauro and the guidance of NASA Glenn personnel.

REFERENCES

1. Haggard, J. B., and Cochran, T. H., *Combust. Sci. Technol.* 5:291 (1972).
2. Bahadori, M. Y., Edelman, R. B., Stocker, D. P., and Olson, S. L., *AIAA J.* 28:236 (1990).
3. Urban, D. L., Yuan, Z. G., Sunderland, P. B., Linteris, G. T., Voss, J. E., Lin, K. C., Dai, Z., Sun, K., and Faeth, G. M., *AIAA J.* 36:1346 (1998).
4. Smooke, M. D., Lin, P., Lam, J., and Long, M. B., *Proc. Combust. Inst.* 23:575–582 (1991).
5. Smooke, M. D., Xu, Y., Zurn, R. M., Lin, P., Frank, J. H., and Long, M. B., *Proc. Combust. Inst.* 24:813–822 (1992).
6. Smooke, M. D., Ern, A., Tanoff, M. A., Valdati, B. A., Mohammed, R. K., Marran, D. F., and Long, M. B., *Proc. Combust. Inst.* 26:2161–2170 (1996).
7. Marran, D. F., "Quantitative Two-Dimensional Laser Diagnostics in Idealized and Practical Combustion Systems," Ph.D. thesis, Yale University, New Haven, CT, 1996.
8. Walsh, K. T., Long, M. B., Tanoff, M. A., and Smooke, M. D., *Proc. Combust. Inst.* 27:615–623 (1998).
9. Bowman, C. T., Hanson, R. K., Davidson, D. F., Gardiner Jr., W. C., Lissianski, V., Smith, G. P., Golden, D. M., Frenklach, M., Wang, H., and Goldenberg, M., *GRI-Mech Version 2.11*, http://www.gri.org, Gas Technology Institute, Des Plaines, IL 1995 (accessed Sept. 2000).
10. Eckbreth, A. C., *Laser Diagnostics for Combustion Temperature and Species, 2nd ed.*, Combustion Science and Technology Book Series, Gordon and Breach, Amsterdam, 1996.
11. Long, M. B., "Multi-Dimensional Imaging in Combusting Flows by Lorenz-Mie, Rayleigh, and Raman Scattering," in *Instrumentation for Flows with Combustion*, (A. M. K. P. Taylor, ed.), Academic Press, London, 1993, pp. 467–508.
12. Walsh, K. T., "Quantitative Characterizations of Coflow Laminar Diffusion Flames in a Normal Gravity and Microgravity Environment," Ph.D. thesis, Yale University, New Haven, CT, 2000.